RSC Advances

ROYAL SOCIETY OF CHEMISTRY

www.rsc.org/advances

Self-assembly of glycinin nanoparticles for delivery of phenolic compounds from *Phyllanthus urinaria*

Yong Liu[1*], Shoulian Wei[1], Miaochan Liao[2], Ling Liu[1] and Yunwei Huang[1]

[1]School of Chemistry and Chemical Engineering, Zhaoqing University, Zhaoqing, P.R. China

[2]Department of Logistics Management, Zhaoqing University, Zhaoqing, PR China

Abstract: The purpose of this work was to fabricate and evaluate glycinin nanoparticles for delivery of phenolic compounds from *Phyllanthus urinaria*. The nanoparticles were prepared using self-assembly method, and three variables, including pH (X_1), glycinin concentration (X_2), and glycinin to phenolic compounds mass ratio (X_3), for the achievement of high encapsulation efficiency of phenolic compounds were optimized using response surface methodology. The statistical analyses show that the independent variables (X_1, X_2) and the quadratic terms (X_1^2, X_2^2 and X_3^2) have significant effect on the encapsulation efficiency. The optimized conditions are X_1 of 4.4, X_2 of 3.2 mg/mL, and X_3 of 6.2:1. Under these conditions, the experimental value is 51.42% (n=3), which is well matched with the predicted value. Scanning electron microscopy (SEM) micrograph and dynamic light scattering (DLS) analyses show that the nanoparticles have an approximately spherical morphology with a smooth surface, and the mean particle size was about 100 nm with a narrow size distribution of 0.318. The release of phenolic compounds shows a faster release at pH 7.4 but a lower release at pH 1.2, and the release mechanism at pH 1.2 and 7.4 is Fickian diffusion and anomalous transport, respectively.

Keywords: *Phyllanthus urinaria*; phenolic compounds; self-assembly; glycinin; nanoparticles.

1. Introduction

Phyllanthus urinaria, commonly called chamberbitter, gripeweed, shatterstone, stonebreaker, or leafflower, is one of the species belonging to the genus *Phyllanthus*

*Corresponding author at: School of Chemistry and Chemical Engineering, Zhaoqing University, Zhaoqing, 526061, P.R. China
Tel.: +86 758 2716357.
E-mail: lygdut@163.com (Yong Liu).

(Euphorbiaceae) and is widely distributed in Southern America and many countries in Asia, such as China, India and Thailand [1-3]. *P. urinaria* has been used as a traditional medicine for the treatment of some diseases including diarrhea, dysentery, hepatitis, edema, infantile malnutrition, acute conjunctivitis, aphthae and antibiotic resistant pyogenic infections [4] because it has many biological and pharmacological activities *in vitro* and *in vivo*, such as antiviral [5,6], hepatoprotective anti-inflammatory [7,8], hypoglycemic and hypocholesterolemic [9], antioxidant [10,11], anti-allodynic and anti-oedematogenic [12], and antibacterial [13] properties. The anticancer effect of *P. urinaria* has been reported in some academic literatures [2,6,14-17], and in recent years there is increasing interest to understand and develop alternative agents from *P. urinaria* compounds for the treatment of hepatitis B virus and liver cancer [1,18-22]. It is believed that the phenolic compounds from *P. urinaria* are one of the main effective substances for the treatment of hepatitis B virus and liver cancer [23-26]. However, in conventional administration, the therapeutic effects of the phenolic compounds are limited due to their poor stability in gastrointestinal tract and limited bioavailability *in vivo*. Moreover, the phenolic compounds' unpleasant taste, like astringency and bitterness, also limits their applications. Therefore, it is very necessary to develop effective methods to overcome these disadvantages.

Nanoencapsulation technology is an effective method to overcome the disadvantages mentioned above [27]. Nanoparticles bearing anticancer drugs have received increasing attention because they not only can improve the stability and bioavailability of the drugs and mask the unpleasant taste of drugs [28], but also can facilitate the drugs to go across critical and specific biological barriers and hit specific targets [29]. Additionally, nanoparticles can prevent the first pass metabolism of the drug molecules through a lymphatic uptake mechanism [30], and are particularly useful for cancer chemoprevention for their enhanced permeability and retention effect [31]. Therefore, significant efforts in recent years have been devoted to fabricate and use nanoparticles to encapsulate drugs for targeted drug delivery and targeted cancer therapy [32].

Molecular self-assembly is the spontaneous organization of molecules due to their mutual interaction (from the noncovalent type) into ordered aggregates (spatial and/or temporal ordering) without external control [33,34], and is the elegant and powerful approach to design nanomaterials [35]. In recent years, proteins and peptides have gained great interest in delivering drugs and bioactive molecules [36-40]. Soy protein is an abundant, renewable, and inexpensive

natural protein, which has gained considerable attention for its potential role in improving risk factors for cardiovascular disease [39]. Glycinin is one of the two major globulins of soy protein, and is sensitive to the pH of solution. Therefore, glycinin nanoparticles can be self-assembled by controlling the pH of glycinin solution.

In this work, glycinin nanoparticles were self-assembled to encapsulate phenolic compounds from *P. urinaria*. The effects of pH, glycinin concentration, and glycinin to phenolic compounds mass ratio on the encapsulation efficiency were investigated, and the response surface methodology (RSM) was employed to optimize these variables for the achievement of high encapsulation efficiency of the phenolic compounds. The structure and properties of the nanoparticles were studied by SEM and DLS, and the release behaviors and release mechanism of the phenolic compounds from the nanoparticles were also investigated in detail.

2. Experimental

2.1 Materials and chemicals

Glycinin (protein content of 91.25%) was prepared according to Nagano [41]. *P. urinaria* was bought from herb stores. Glutaraldehyde (GA, 50% solution) was purchased from Aladdin (Shanghai, China). Other reagents were analytical grade and used as received.

2.2 Extraction of phenolic compounds from *P. urinaria*

The dry *P. urinaria* was powdered by a pulverizer (XS-10B, Longxin, China) and then passed through an 80 mesh sieve. Fifty grams of the *P. urinaria* powders were extracted twice with 500 ml of 60 % ethanol at room temperature for one day. The extracts were filtered through a filter paper with 0.22 μm pore size and concentrated by evaporating the solvent under the reducing pressure. The concentrated liquid was finally freeze-dried by a freeze dryer (LL3000, Heto, Germany) to obtain the powders of phenolic compounds. The phenolic compounds obtained under ethanol extraction are mainly composed of gallic acid, corilagin, geraniin, ellagic acid, brevifolin, quercetin, luteolin and kaempferol [23,42-44].

2.3 Determination of total phenolic content

The total phenolic content was determined using ferrous tartrate method [45] with a slight modification. One milliliter of sample solution was transferred into a 25 mL volumetric flask to react with 5 mL solution dye (0.1 g ferrous sulfate and 0.5 g potassium sodium tartrate

tetrahydrate dissolved in 100 mL distilled water), 4 mL distilled water and 15 mL buffer solution (0.067 mol/L potassium phosphate, pH 7.5). The mixture was kept for 5 min for color development. The absorbance was measured at 540 nm by a UV-vis spectrophotometer (UVmini-1240, Shimadzu, Japan), using a blank solution prepared with distilled water replacing the sample solution. The total phenolic content was calculated as gallic acid equivalent from the calibration curve of gallic acid standard solutions (0-50 mg/L).

2.4 Self-assembly of phenolic compounds loaded glycinin nanoparticles

A certain concentration of glycinin solution was prepared by dispersing the glycinin powder in an aqueous solution with pH of 8.0 to completely dissolution with stirring, whereas a certain concentration of phenolic solution was prepared by dissolving the phenolic powders in distilled water. While constantly stirring the solution, phenolic compounds were added and the mixture was kept stirring for 10 min, and then the pH of the mixture was adjusted with 2 mol/L HCl solution to form nanoparticles. Then glutaraldehyde (30 μg/mg glycinin) was added to cross-link the nanoparticles for 6 h under stirring constantly. Finally, the mixture was centrifuged at 12000 g for 20 min. The precipitate was freeze-dried for 24 h by a freeze dryer (LL3000, Heto, Germany) to obtain the glycinin nanoparticles loaded with phenolic compounds, whereas the phenolic content in the supernatant was determined using the established standard curve to calculate the encapsulation efficiency (EE) of the phenolic compounds in the nanoparticles. The EE was calculated using the following equation:

$$\mathrm{EE}\ (\%) = \frac{\text{total phenols - free phenols}}{\text{total phenols}} \times 100 \quad (1)$$

2.5 Optimum design

A three-level-three-factor, Box-Behnken design (BBD) was employed to determine the best combination of variables for the encapsulation efficiency based on the results of preliminary single-factor-test. pH (X_1), glycinin concentration (X_2), and glycinin to phenolic compounds mass ratio (X_3) were the independent variables, and their coded and uncoded levels were presented in Table 1. The encapsulation efficiency (Y) taken as the response for the design experiment was given in Table 2. Experimental data were fitted to a quadratic polynomial model and the model was explained by the following quadratic equation:

$$Y = A_0 + \sum_{i=1}^{3} A_i X_i + \sum_{i=1}^{3} A_{ii} X_i^2 + \sum_{i=1}^{2} \sum_{j=i+1}^{3} A_{ij} X_i X_j \quad (2)$$

Where Y is the dependent variable; A_0, A_i, A_{ii}, and A_{ij} are the regression coefficients for intercept, linearity, square and interaction, respectively; X_i and X_j are the independent variables.

2.6 Surface morphology analysis

Scanning electron microscopy (SEM) was performed to examine the surface morphology of the phenolic compounds-loaded nanoparticles. The freeze-dried nanoparticles loaded with phenolic compounds were first sputter-coated with conductive carbon, and then the morphology was examined using SEM (Supra 55, Zeiss, Germany) with an acceleration voltage of 20 kV.

2.7 Particle size measurement

The particle size and size distribution of the phenolic compounds-loaded nanoparticles were performed by dynamic light scattering (DLS) using a particle size analyzer (ZS90, Malvern, UK).

2.8 In vitro drug release study

The glycinin nanoparticles loaded with phenolic compounds were put in a dialysis bag and the dialysis bag was clamped by a clip. Then, the dialysis bag with the nanoparticles was immersed in a conical vial containing 50 mL of buffer solution. The vial was closed and incubated in a thermostatic shaker (SKY100C, Sukun, China) with a speed of 60 rpm at 37 °C. At given time intervals, 1 mL of the solution was taken out to measure the release amount of phenolic compounds according to the ferrous tartrate method, and 1 mL of fresh buffer solution was put back into the same vial. The cumulative release of phenolic compounds was calculated with the following equation:

$$\text{Cumulative release of phenolic compounds } (\%) = \frac{M_t}{M_0} \times 100 \quad (3)$$

Where M_t is the cumulative amount of phenolic compounds released at time t, and M_0 is the initial amount of phenolic compounds loaded.

2.9 Statistical analysis

All the data were determined in triplicate and the results were averaged. Design Expert

software version 8.0.6 (Stat-Ease, Minneapolis) was employed for the regression analysis and the optimization.

3. Results and Discussion

3.1 Effect of pH on encapsulation efficiency of phenolic compounds

Self-assembly of glycinin nanoparticles for encapsulation of phenolic compounds from *P. urinaria* was carried out using pH from 3.5 to 5.5, while other parameters were as follows: glycinin concentration 3 mg/mL and glycinin to phenolic compounds mass ratio 4:1. The effect of pH on encapsulation efficiency of phenolic compounds is shown in Fig. 1A. When pH increases, the variance of encapsulation efficiency is relatively rapid and reaches a maximum at pH 4.5 and then decreases. When the pH of solution is near isoelectric point (pI) of glycinin, the net charges on the protein molecules are almost zero. At this time, the protein molecules aggregate to form particles due to the weak mutual repulsion forces between the protein molecules and the phenolic compounds are simultaneously encapsulated in the particles. Moreover, the pH of solution is nearer to pI, the more particles are formed, and the more phenolic compounds are encapsulated. Therefore, pH 4.5-5.0 is favorable for encapsulating the phenolic compounds.

3.2 Effect of glycinin concentration on encapsulation efficiency of phenolic compounds

The encapsulation of phenolic compounds from *P. urinaria* was carried out at different glycinin concentration of 1, 2, 3, 4 and 5 mg/mL, while other parameters were as follows: pH 4.5 and glycinin to phenolic compounds mass ratio 4:1. The effect of glycinin concentration on encapsulation efficiency of phenolic compounds is shown in Fig. 1B. The variance of encapsulation efficiency increases first and then decreases with the increase of glycinin concentration, and peaks at 3 mg/mL. As the glycinin concentration increases, the number of glycinin particles per unit volume in the solution increases, resulting in more phenolic compounds encapsulated in the particles and consequently the higher encapsulation efficiency. When the glycinin concentration exceeds 3 mg/mL, the mean separation distance between the particles decreases and the collisions between particles are more frequent, resulting in larger particles formed in the solution. The formation of larger particles makes the number of particles per unit volume in the solution decreases, resulting in less phenolic compounds encapsulated in the larger particles and consequently the lower encapsulation efficiency.

Therefore, the glycinin concentration of 3 mg/mL is good for encapsulating the phenolic compounds.

3.3 Effect of glycinin to phenolic compounds mass ratio on encapsulation efficiency of phenolic compounds

The encapsulation of phenolic compounds from *P. urinaria* was carried out at different glycinin to phenolic compounds mass ratio in the range of 2:1 to 10:1, while pH and glycinin concentration were fixed at 4.5 and 3 mg/mL, respectively. The effect of glycinin to phenolic compounds mass ratio on encapsulation efficiency of phenolic compounds is shown in Fig. 1C. As the mass ratio increases, the encapsulation efficiency increases initially with a maximum achieved at 6:1 and then starts slightly decreasing. This phenomenon may be attributed to the critical concentration of phenolic compounds in the solution. The lower mass ratio, the higher concentration of phenolic compounds in the solution for the glycinin concentration fixed at 3 mg/mL; while the higher mass ratio, the lower content of phenolic compounds. Below the critical concentration, at lower mass ratio, the number of particles is not sufficient for encapsulating the phenolic compounds, leading to lower encapsulation efficiency; with the increase in the mass ratio, the concentration of phenolic compounds decreases and the encapsulation efficiency increases. But above critical concentration, the mass ratio further increases, the encapsulation efficiency decreases for the drastically decrease in the concentration of phenolic compounds. Therefore, the mass ratio of 6:1 is sufficient for encapsulating the phenolic compounds.

3.4 Optimization of parameters for encapsulation efficiency of phenolic compounds

Table 2 shows the process variables and experimental data of 15 runs containing 3 replicates at center point. By applying multiple regression analysis on the experimental data, the model for the response variable could be expressed by the following quadratic polynomial equation in the form of coded values:

$$Y=51.26 - 1.10X_1 + 0.83X_2 + 0.69X_3 - 3.20X_1^2 - 2.16X_2^2 - 4.77X_3^2 + 0.26X_1X_2 + 0.095X_1X_3 + 0.39X_2X_3 \quad (4)$$

Analysis of variance (ANOVA) for the model is shown in Table 3. The determination coefficient (R^2=0.9788) indicates that only 2.12 % of the total variations are not explained by the model. For a good statistical model, the adjusted determination coefficient (R^2_{adj}) should be

close to R^2. As shown in Table 3, R^2_{adj} (0.9407) is close to R^2, which confirms that the model is highly significant. The lack of fit test determines whether the selected model is adequate to explain the experimental data, or whether another model should be reselected. The value of lack of fit test (0.0719) is higher than 0.05, which is not significant relative to the pure error and indicates that the fitting model is adequate to describe the experimental data. At the same time, a relatively low value of coefficient of variation (CV) (1.72) indicates a better precision and reliability of the experimental values. Therefore, the model is adequate for prediction in the range of experimental variables.

The significance of each coefficient measured using *p*-value and *F*-value is listed in Table 4. Smaller *p*-value and greater *F*-value mean the corresponding variables would be more significant. The *p*-value of the model is 0.0012, which indicates that the model is significant and can be used to optimize the encapsulation variables. The two independent variables (X_1, X_2) and three quadratic terms (X_1^2, X_2^2 and X_3^2) significantly affect the encapsulation efficiency within a 96% confidence interval. But the interaction between pH (X_1), glycinin concentration (X_2) and glycinin to phenolic compounds mass ratio (X_3) is not significant ($p > 0.05$). Meanwhile, pH (X_1) is the most significant factor affecting the encapsulation efficiency.

3D response surface and 2D contour plots are the graphical representations of regression equation and are very useful to judge the relationship between independent and dependent variables. Different shapes of the contour plots indicate whether the mutual interactions between the variables are significant or not. Circular contour plot means the interactions between the corresponding variables are negligible, while elliptical contour suggests the interactions between the corresponding variables are significant [46]. The three-dimensional representation of the response surfaces and two-dimensional contours generated by the model are shown in Figs. 2-4. In these three variables, when two variables are depicted in three-dimensional surface plots, the third variable is fixed at zero level.

As shown in Fig. 2, encapsulation efficiency increases rapidly when pH (X_1) and glycinin concentration (X_2) increase in the range of 3.50 to 4.42 and 1.00 to 3.19 mg/mL, respectively; but beyond 4.42 and 3.19 mg/mL, encapsulation efficiency also decreases quickly. This demonstrates that the effect of pH (X_1) and glycinin concentration (X_2) on encapsulation efficiency is significant and is in good agreement with the results in Table 4. The circular

contour plots in Fig. 2 mean that the interaction between the two variables is not significant, which also agrees with the results in Table 4. From Fig. 3, both pH (X_1) and glycinin to phenolic compounds mass ratio (X_3) have quadratic effect on encapsulation efficiency. Encapsulation efficiency increases at first and then decreased quickly with increasing of the two parameters, and maximum encapsulation efficiency is achieved when pH (X_1) and glycinin to phenolic compounds mass ratio (X_3) are 4.42 and 6.16:1, respectively. It can be seen that the mutual interactions between pH (X_1) and glycinin to phenolic compounds mass ratio (X_3) are not significant due to the circular contour plots shown in Fig. 3, which is also confirmed by the results in Table 4. It is obvious in Fig. 4 that encapsulation efficiency increases with increasing of glycinin concentration (X_2) from 1.00 to 3.19 mg/mL and decreases slowly after 3.19 mg/mL; while encapsulation efficiency increases rapidly with increasing of glycinin to phenolic compounds mass ratio (X_3) from 2.00:1 to 6.16:1 and decreases rapidly after 6.16:1. The circular contour plots in Fig. 4 suggest that the interactions between the two variables are not significant, which is in agreement with the results in Table 4.

3.5 Verification of the model

The suitability of the model equation for predicting the optimum response values are tested using the selected optimum conditions. The optimum conditions are pH (X_1) of 4.42, glycinin concentration (X_2) of 3.19 mg/mL, and glycinin to phenolic compounds mass ratio (X_3) of 6.16:1, under which the predicted value is 51.45%. The model is experimentally verified at pH (X_1) of 4.4, glycinin concentration (X_2) of 3.2 mg/mL, and glycinin to phenolic compounds mass ratio (X_3) of 6.2:1, under which the experimental value is 51.42±0.09% (n=3), agreeing closely with the predicted value and consequently indicating the RSM model is satisfactory and accurate. The high encapsulation efficiency may be primarily related to the formation of hydrogen bonds between phenolic hydroxyl groups of phenolic compounds and amino groups and carboxyl groups of glycinin, resulting in more phenolic compounds encapsulated in the nanoparticles or adsorbed on the surface of nanoparticles.

3.6 Morphology analysis and size distribution

The morphology of phenolic compounds-loaded nanoparticles self-assembled according to the optimum conditions was investigated using SEM (Fig. 5A). The nanoparticles have an

approximately spherical morphology with a smooth surface, and the size of the nanoparticles measured from SEM is in the range of 60-110 nm and the mean size is about 80 nm. The size distribution of the phenolic compounds-loaded nanoparticles was also calculated by dynamic light scattering (DLS) measurement (Fig. 5B). The mean size of the nanoparticles observed from DLS is found to be about 100 nm with a polydispersity index (PDI) of 0.318. The low PDI clearly indicates a narrow size distribution of the prepared nanoparticles. Compared with the particle size observed from SEM and DLS, the particle size obtained from SEM is 20 % lower than those measured using DLS. This difference is due to the fact that DLS measured the particle size in solution, whereas SEM analyzed the particle size in freeze dried state which caused the shrinkage of nanoparticles by the cast-drying process in the vacuum environment [47-49].

3.7 In vitro drug release

The kinetic release profiles of phenolic compounds at different pHs at 37 °C are shown in Fig. 6. The release of phenolic compounds from the nanoparticles at pH 7.4 is faster than that at pH 1.2. In the first 90 min, 72.12 % and 43.63 % of phenolic compounds is released at pH of 1.2 and 7.4, respectively. The high release effect in the first 90 min is due to the release of phenolic compounds that are associated with the adsorption of phenolic compounds on the surface of nanoparticles owing to the hydrogen bonds and those that are easy to separate from the surface of nanoparticles by constant shaking in the shaker; and it is also attributed to the release of phenolic compounds that are incorporated shallower into the nanoparticles. The different release effect at pH 1.2 and 7.4 may be mainly related to the release environment. As pH (1.2) is below pI of glycinin, carboxyl acid groups along the glycinin backbone form hydrogen bonds with polar groups, resulting in a more compact network structure in the nanoparticles. This compact structure makes the water molecules diffuse into the nanoparticles slower, leading to the slower dissolution of phenolic compounds. At the same time, the compact structure also causes the increase of the outward diffusion resistance for phenolic compounds, resulting in the slower release of phenolic compounds. But as pH (7.4) is above pI of glycinin, the electrostatic repulsion between carboxyl anion groups along the glycinin backbone makes the nanoparticles have an expanding structure, causing the faster diffusion of water molecules into the nanoparticles and consequently the faster dissolution of

phenolic compounds. Also, the expanding structure can decrease the outward diffusion resistance for phenolic compounds, leading to the faster release of phenolic compounds. After the fast release, a subsequent sustained release is observed. This is attributed to the release of phenolic compounds that are incorporated deeper into the nanoparticles, resulting in a longer distance for phenolic compounds release; and it is also due to the release of phenolic compounds that are combined with glycinin through hydrogen bonds, leading to the sustained release.

In order to investigate the release mechanism of phenolic compounds from the nanoparticles, the release data were analyzed by fitting the following equations [50]:

$$\frac{M_t}{M_\infty} = kt^n \quad (5)$$

Where M_t/M_∞ is the fractional release of phenolic compounds at the time t, k is the release constant and n is the characteristic exponent related to the release mechanism of phenolic compounds. For spherical systems, $n \leq 0.43$, $0.43 < n < 0.85$, $n = 0.85$, and $n > 0.85$ is for the release mechanism of Fickian diffusion, anomalous (non-Fickian) transport, Case II transport (zero-order diffusion) and super Case II transport, respectively. $M_t/M_\infty \leq 0.6$ should only be used in this equation.

The values of n obtained from the slope of the plot of $\ln(M_t/M_\infty)$ versus $\ln t$ for phenolic compounds release at pH 1.2 and 7.4 are 0.43 (R^2=0.96269) and 0.68 (R^2=0.99781), respectively. These results indicate that the release mechanism of phenolic compounds at pH 1.2 and 7.4 is Fickian diffusion and anomalous transport, respectively, and the diffusion rate of phenolic compounds at pH 1.2 is lower than that at pH 7.4, which is consistent with the results in Fig. 6.

4. Conclusions

The glycinin nanoparticles for encapsulation of phenolic compounds from *P. urinaria* were fabricated using self-assembly method and the self-assembled condition for encapsulation efficiency of phenolic compounds was optimized by RSM. The results show that the pH and glycinin concentration are significant and a high correlation of quadratic model obtained is satisfactory and accurate to predict the encapsulation efficiency. The optimized conditions are as follows: pH 4.4, glycinin concentration 3.2 mg/mL, and glycinin to phenolic compounds

mass ratio 6.2:1. Under these conditions, the encapsulation efficiency is 51.42% (n=3). The nanoparticles are approximately spherical with the mean particle size in 100 nm. The release of phenolic compounds from the nanoparticles at pH 7.4 is faster than that at pH 1.2, and the release mechanism at pH 1.2 and 7.4 is Fickian diffusion and anomalous transport, respectively, according to the Ritger-Peppas model.

Acknowledgement

This work is financially supported by the Natural Science Foundation of Guangdong Province (No. S2012040007710), the Characteristic Innovation Project of Education Department of Guangdong Province (No. 2014TSCX) and the Natural Science Foundation of Zhaoqing University (No. 201201).

References

1 N. Chudapongse, M. Kamkhunthod and K. Poompachee, *J. Ethnopharmacol.*, 2010, **130**, 315.

2 S. T. Huang, R. C. Yang, P. N. Lee; S. H. Yang, S. K. Liao, T. Y. Chen and J. H. S. Pang, *Int. Immunopharmacol.*, 2006, **6**, 870.

3 K. H. Lu, H. W. Yang, C. W. Su, K. H. Lue, S. F. Yang and Y. S. Hsieh, *Food Chem. Toxicol.*, 2013, **52**, 193.

4 S. T. Huang, C. Y. Wang, R. C. Yang, H. T. Wu, S. H. Yang, Y. C. Cheng and J. H. S. Pang, *Evid. Based Complement. Alternat. Med.*, 2011, 215035.

5 D. K. Hau, R. Gambari, R. S. Wong, *Phytomedicine*, 2009, **16**, 751.

6 M. Wang, H. Cheng, Y. Li, L. Meng, G. Zhao and K. Mai, *J. Lab. Clinical Med.*, 1995, **126**, 350.

7 C. A. L. Kassuya, D. F. P. Leite, L. V. de-Melo, V. L. C. Rehder and J. B. Calixto, *Planta Med.*, 2005, **71**, 721.

8 A. K. Kiemer, T. Hartung, C. Huber and A. M. Vollmar, *J. Hepatol.*, 2003. **38**, 289.

9 A. A. Adeneye, O. O. Amole and A. K. Adeneye, *Fitoterapia*, 2006, **77**, 511.

10 R. Krithika, R. Mohankumar, R. J. Verma, P. S. Shrivastav, I. L. Mohamad, P. Gunasekaran and S. Narasimhan, *Chem. Biol. Interactions*, 2009, **181**, 351.

11 S. Y. Lin, C. C. Wang, Y. L. Lu, W. C. Wu and W. C. Hou, *Food Chem. Toxicol.*, 2008, **46**,

2485.

12 C. A. L. Kassuya, A. A. Silvestre, V. L. G. Rehder and J. B. Calixto, *Eur. J. Pharmacol.*, 2003, **478**, 145.

13 C. H. Lai, S. H. Fang, Y. K. Rao, M. Geethangili, C. H. Tang, Y. J. Line, C. H. Hung, W. C. Wang and Y. M. Tzeng, *J. Ethnopharmacol.*, 2008, **118**, 522.

14 R. Bharali, J. Tabassum and M. R. Azad, *Indian J. Exp. Biol.*, 2003, **41**, 1325.

15 S. T. Huang, R. C. Yang, M. Y. Chen and J. H. Pang, *Life Sci.*, 2004, **75**, 339.

16 S. T. Huang, R. C. Yang and J. H. S. Pang, *Am. J. Chinese Med.*, 2004, **32**, 175.

17 G. Powis and D. Moore, *J. Chromatogr.*, 1985, **342**, 129.

18 S. T. Huang, J. H. Pang and R. C. Yang, *Chang Gung Med. J.*, 2010, **33**, 477.

19 H. Li, C. T. Zhang, H. Y. Gu, C. J. Chen and J. Y. Qu, *China Med. Eng.*, 2011, **19**, 7.

20 M. Y. Liang, C. Q. Li, X. L. Wang, M. Zhao and X. H. Li, *China Trop. Med.*, 2012, **12**, 6.

21 B. Tan, X. Xu, J. Luo, J. Guo and W. Xu, *China Med. Her.*, 2013, **10**, 15.

22 X. Xia, M. Zhao, C. Li, X. Li and F. Zhao, *J Guangzhou Univ. Tradit. Chinese Med.*, 2013, **30**, 690.

23 C. Lin, Y. B. Yuan, L. Z. Zhang and R. B. Shi, *Chinese Tradit. Her. Drug*., 2012, **43**, 2055.

24 K. F. Wang, C. Lin, L. F. Wu, S. W. Li and L. Z. Zhang, *Chinese J. Exp. Tradit. Med. Formulae*, 2013, **19**, 110.

25 M. Xu, Z. J. Zha, X. L. Qin, X. L. Zhang, C. R. Yang and Y. J. Zhang, *Chem. Biodivers.*, 2007, **4**, 2246.

26 X. Y. Yan, M. Sun, G. G. Yang, K. S. Bi and X. H. Chen, *J. Shenyang Pharm. Univ.*, 2012, **29**, 45.

27 I. S. Santos, B. M. Ponte, P. Boonme, A. M. Silva and E. B. Souto, Biotechnol. Adv., 2013, **31**, 514.

28 E. Roger, F. Lagarce, E. Garcion and J. P. Benoit, *Nanomedicine*, 2010, 5, 287.

29 S. Yu, J. Hu, X. Pan, P. Yao and M. Jiang, *Langmuir*, 2006, **22**, 2754.

30 C. N. Grama, D. D. Ankola and M. N. V. R. Kumar, *Curr. Opin. Colloid Inter. Sci.*, 2011, **16**, 238.

31 I. A. Siddiqui, V. M. Adhami, D. J. Bharali, B. B. Hafeez, M. Asim, S. I. Khwaja, N. Ahmad, H. Cui, S. A. Mousa and H. Mukhtar, *Cancer Res.*, **69**, 1712 2009.

32 L. Brannon-Peppas and J. O. Blanchette, *Adv. Drug Deliver. Rev.*, 2012, **64**, 206.

33 A. C. Mendes, E. T. Baran, R. L. Reis and H. S. Azevedo, *Wiley Interdiscip. Rev. Nanomed. Nanobiotechnol.*, 2013, **5**, 582.

34 G. M. Whitesides and B. Grzybowski, *Science*, 2002, **295**, 2418.

35 N. P. King, W. Sheffler, M. R. Sawaya, B. S. Vollmar, J. P. Sumida, I. André, T. Gonen, T. O. Yeates and D. Baker, *Science*, 2012, **336**, 1171.

36 A. Nesterenko, I. Alric, F. Silvestre and V. Durrieu, *Ind. Crop. Prod.*, 2013, **42**, 469.

37 M. H. A. El-Salam and S. El-Shibiny, *Int. J. Dairy Technol.*, 2012, **65**, 13.

38 A. MaHam, Z. Tang, H. Wu, J. Wang and Y. Lin, *Small*, 2009, **5**, 1706.

39 S. S. Gupta and M. Ghosh, *J. Food Eng.*, 2014, **121**, 64.

40 K. Matsuurua, *RSC Adv.*, 2014, **4**, 2942.

41 T. Nagano and M. Tokita, *Food Hydrocolloid.*, 2011, **25**, 1647.

42 E. S. Mahdi, A. M. Noor, M. H. Sakeena, G. Z. Abdullah, M. Abdulkarim and M. A. Satta, *Afr. J. Pharm. Pharmacol.*, 2011, **5**, 1967.

43 T. Zhao, Y. Jin and Q. H. Jing, *West China J. Pharm. Sci.*, 2013, **28**, 207.

44 Y. B. Yuan, L. Z. Zhang, Y. J. Guo and Y. Y. Ba, *J. Beijing Univ. Tradit. Chinese Med.*, 2009, **32**, 56.

45 N. Turkmen, F. Sari and Y. S. Velioglu, *Food Chem.*, 2006, **99**, 835.

46 R. V. Muralidhar, R. R. Chirumamila, R. Marchant and P. Nigam, *Biochem. Eng. J.*, 2001, **9**, 17.

47 Z. Li, S. S. Percival, S. Bonard and L. Gu, Mol. *Nutr. Food Res.*, 2011, **55**, 1096.

48 T. Mirshahi, J. M. Irache, J. Gueguen and A. M. Orecchioni, *Drug Dev. Ind. Pharm.*, 1996, **22**, 841.

49 T. Zou, S. L. Li, X. Z. Zhang, X. J. Wu, S. X. Cheng and R. X. Zhuo, *J. Polym. Sci. A: Polym. Chem.*, 2007, **45**, 5256.

50 R. E. Domaratzki and A. Ghanem, *J.Appl. Polym. Sci.*, 2013, **128**, 2173.

Table 1 Independent variables and their levels for Box-Behnken design

Independent variables	Levels		
	-1	0	1
pH (X_1)	4.0	4.5	5.0
Glycinin concentration (X_2) (mg/mL)	2.0	3.0	4.0
Glycinin to phenolic compounds mass ratio	4:1	6:1	8:1

Table 2 Box-Behnken design for independent variables and their encapsulation efficiency

Run	X_1 (pH)	X_2 (Glycinin concentration, mg/mL)	X_3 (Glycinin to phenolic compounds mass ratio)	EE (%)
1	0	-1	1	43.15
2	1	-1	0	43.95
3	0	0	0	51.41
4	0	1	-1	44.71
5	1	0	1	43.36
6	0	1	1	46.65
7	-1	1	0	47.33
8	0	-1	-1	42.78
9	-1	0	1	44.81
10	0	0	0	50.94
11	-1	-1	0	47.23
12	-1	0	-1	43.41
13	1	1	0	45.07
14	0	0	0	51.42
15	1	0	-1	41.58

Table 3 Analysis of variance for fitted quadratic model of encapsulation efficiency of phenolic compounds

Source	Sum of squares	Degree of freedom	Mean square	*F*-value	*p*-value (Prob. > *F*)
Model	143.18	9	15.91	25.67	0.0012
Residual	3.1	5	0.62		
Lack of fit	2.95	3	0.98	13.06	0.0719
Pure error	0.15	2	0.075		
Cor. total	146.28	14			

R^2=0.9788; R^2_{adj}=0.9407; C.V.%=1.72.

Table 4 Regression coefficients estimate and their significance test for quadratic model

Source	Sum of squares	Degree of freedom	Mean square	*F*-value	*p*-value (Prob. > *F*)
X_1	9.72	1	9.72	15.69	0.0107
X_2	5.53	1	5.53	8.92	0.0306
X_3	3.77	1	3.77	6.08	0.0568
X_1^2	37.74	1	37.74	60.89	0.0006
X_2^2	17.3	1	17.3	27.91	0.0032
X_3^2	84	1	84	135.52	< 0.0001
X_1X_2	0.26	1	0.26	0.42	0.5457
X_1X_3	0.036	1	0.036	0.058	0.8189
X_2X_3	0.62	1	0.62	0.99	0.3645

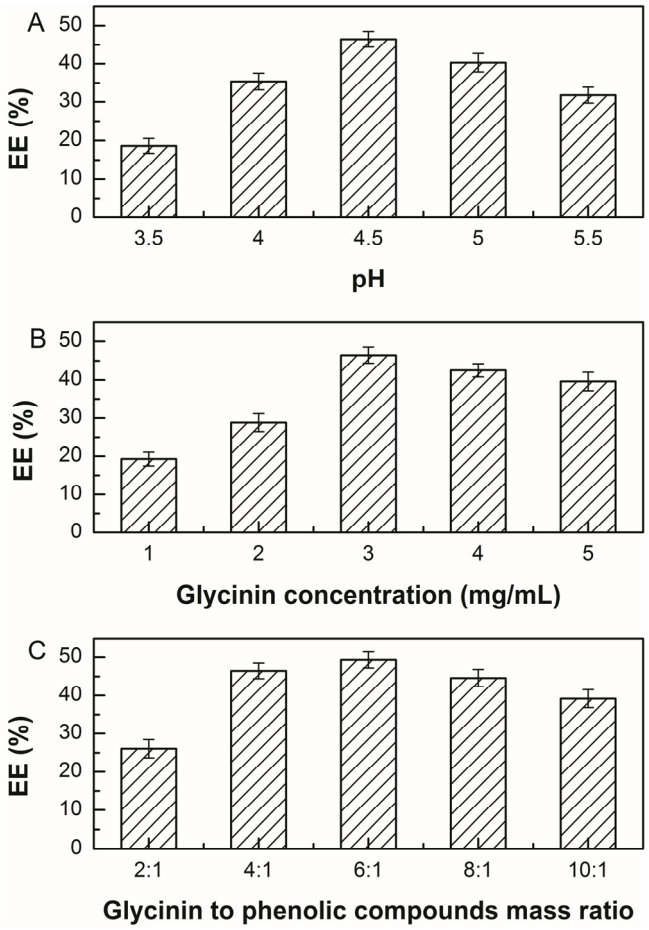

Fig. 1 Effect of different variables on encapsulation efficiency of phenolic compounds.

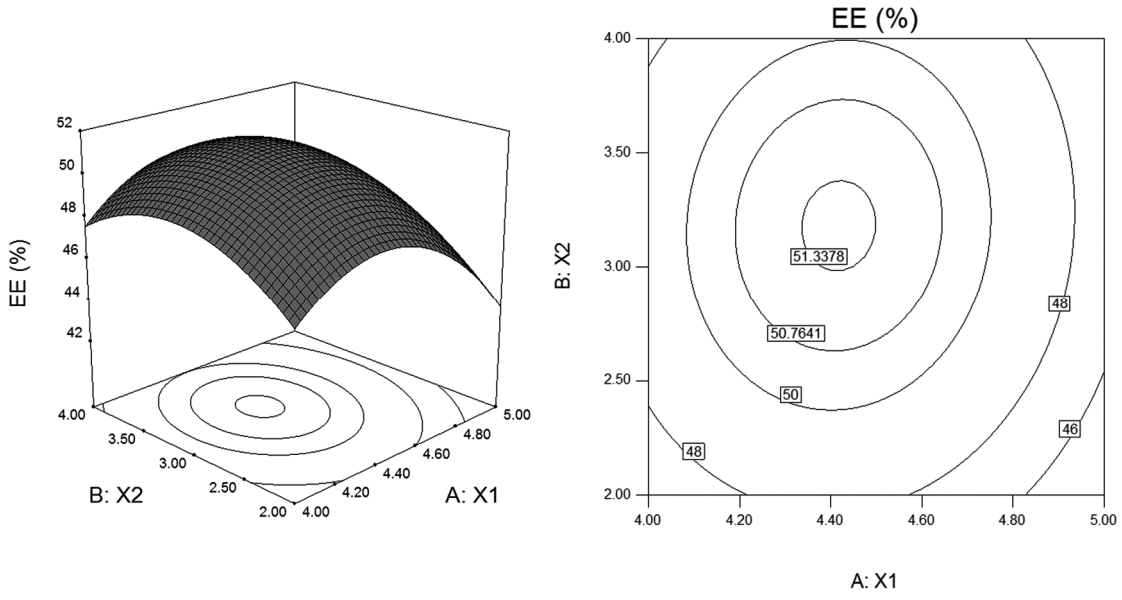

Fig. 2 Response surface and contour plots showing effect of pH (X_1) and glycinin concentration (X_2).

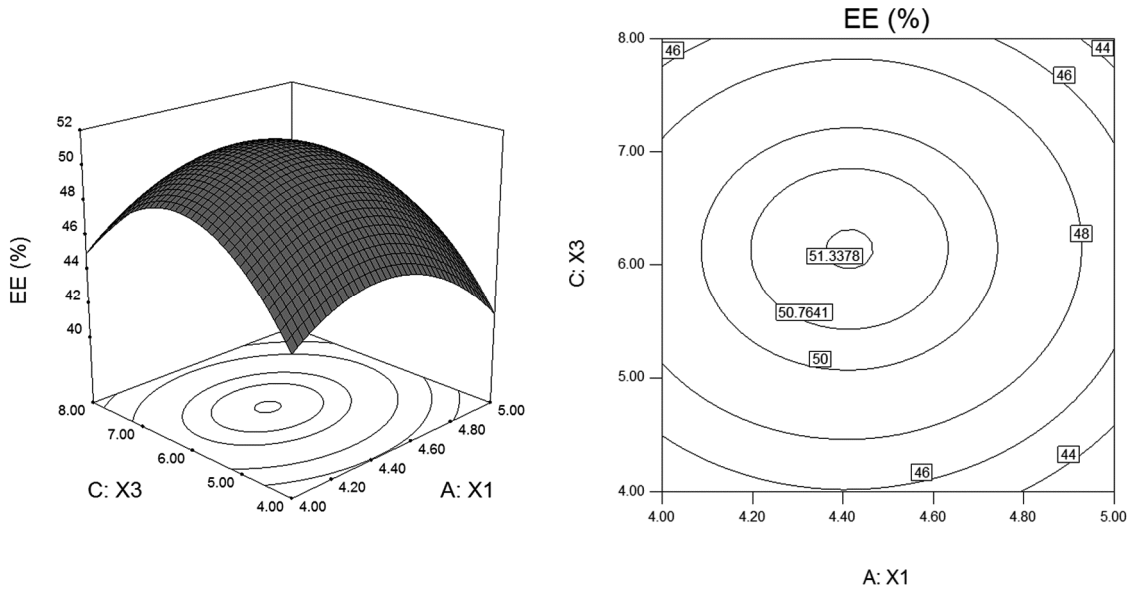

Fig. 3 Response surface and contour plots showing effect of pH (X_1) and glycinin to phenolic compounds mass ratio (X_3).

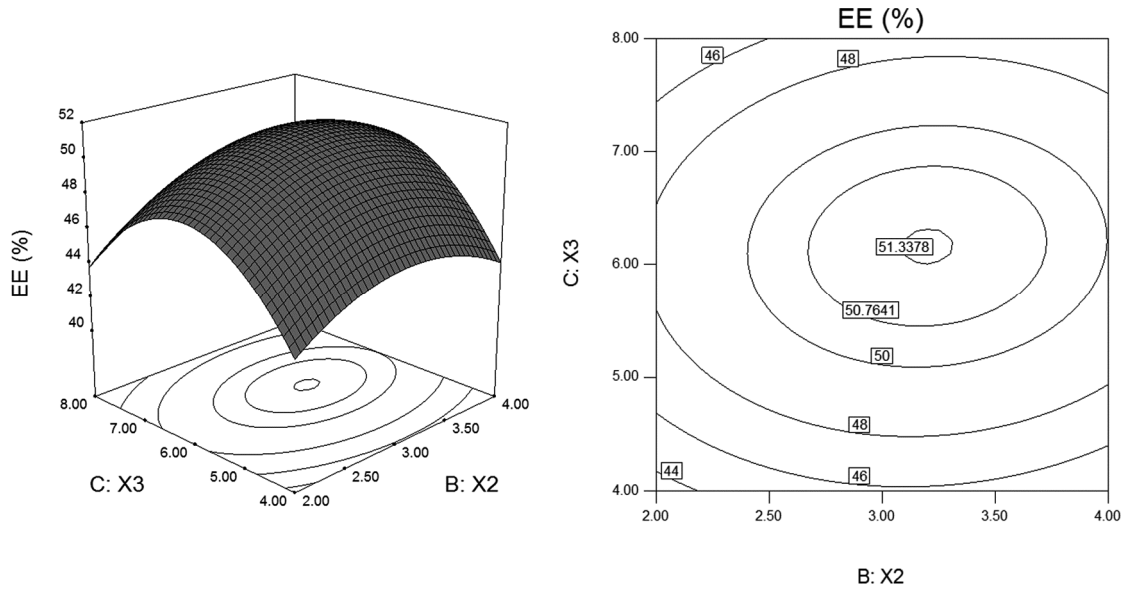

Fig. 4 Response surface and contour plots showing effect of glycinin concentration (X_2) and glycinin to phenolic compounds mass ratio (X_3).

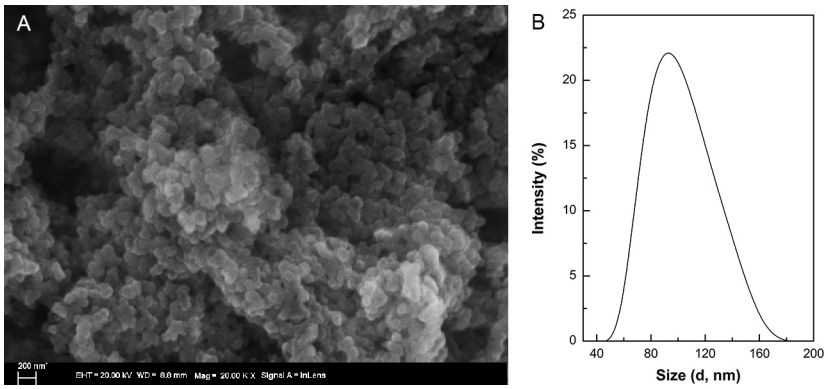

Fig. 5 SEM micrograph (a) and particle size distribution (b) of phenolic compounds-loaded nanoparticles.

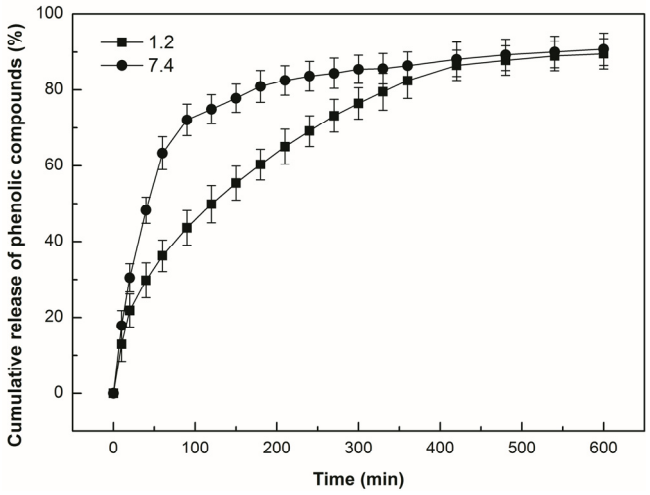

Fig. 6 Release profiles of phenolic compounds from nanoparticles as a function of time.

A table of contents entry

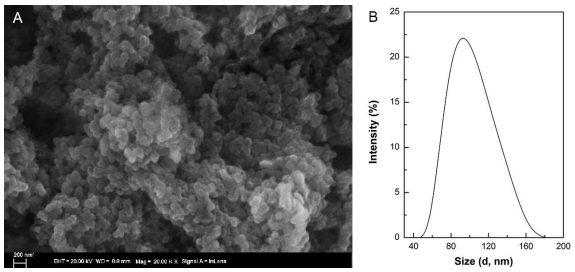

Glycinin nanoparticles for delivery of phenolic compounds from *Phyllanthus urinaria*.